Appl Nanosci (2012) 2:429–436
DOI 10.1007/s13204-012-0060-5

ORIGINAL ARTICLE

Synthesis and characterization of TiO_2/SiO_2 nano composites for solar cell applications

D. Arun Kumar · J. Merline Shyla · Francis P. Xavier

Received: 26 October 2011 / Accepted: 11 January 2012 / Published online: 21 January 2012

Abstract The use of titania–silica in photocatalytic process has been proposed as an alternative to the conventional TiO_2 catalysts. Mesoporous materials have been of great interest as catalysts because of their unique textural and structural properties. Mesoporous TiO_2, SiO_2 nanoparticles and TiO_2/SiO_2 nanocomposites were successfully synthesized by sol–gel method using titanium (IV) isopropoxide, tetra-ethylorthosilicate as starting materials. The synthesized samples are characterized by X-ray diffraction, UV–Vis spectroscopy, Fourier transform infrared spectroscopy, Brunauett–Emmett–Teller and field-dependent photoconductivity. The UV–Vis spectrum of as-synthesized samples shows similar absorption in the visible range. The crystallite size of the as-synthesized samples was calculated by Scherrer's formula. The BET surface area for TiO_2/SiO_2 nanocomposite is found to be 303 m^2/g and pore size distribution has average pore diameter about 10 nm. It also confirms the absence of macropores and the presence of micro and mesopores. The field-dependent photoconductivity of TiO_2/SiO_2 nanocomposite shows nearly 300 folds more than that of TiO_2 nanoparticle for a field of 800 V/cm.

Keywords Nano TiO_2 · Nano SiO_2 · Nanocomposites · Sol–gel · Photoconductivity

Introduction

Nanoclusters of metals and semiconductors are more and more considered as building blocks of future technology. This is due to the size of these particles. Nano crystalline TiO_2 has attracted continuous attention due to its versatile applications in optical devices, sensors, catalysis and photocatalysis etc. (Rufen and Huating 2011). In particular, nanosized TiO_2 has many advantages in the dye-sensitized solar cells. With regards to nanocrystalline TiO_2, the optical properties have been tentatively studied in recent years and some interesting results obtained. The use of large surface area semiconductor for materials in dye-sensitized solar cells (DSSC) is necessary to provide sufficient light absorption and charge separation which are the two critical stages in the solar–electric energy conversion. The mesoporous nano TiO_2/SiO_2 composite is a promising area due to optimum porous size. Nanosized TiO_2 has been fabricated using sol–gel, sputtering, combustion flame, and thermal plasma (Zhang and Xu 2004; San Vicente et al. 2001). Although the sol–gel method is considered as a suitable method to synthesize ultra-fine particles, this method needs a large quantity of solution, longer processing time and heat treatment for crystallization since amorphous TiO_2 has a very little photocatalytic activity. The photo catalytic efficiency of Titania (TiO_2) depends highly on particle size and surface area of the material (Hakki et al. 2009; Ohno et al. 2009). The efficiency of TiO_2 for dye-sensitized solar cells (DSSC) is highly depending on particle size and surface area. Commercially, TiO_2 is available with surface area of around 60 m^2/g. The surface area has further more increased by forming composite with SiO_2.

In this work, TiO_2, SiO_2 nanoparticles and TiO_2/SiO_2 nanocomposites were prepared by a novel and simple route. The TiO_2, SiO_2 nanoparticles were synthesized by sol–gel method using titanium isopropoxide and tetra methyl orthosilicate as starting material. The present work aims at studying the structural, optical and electrical

D. Arun Kumar (✉) · J. Merline Shyla · F. P. Xavier
Department of Physics, Loyola Institute of Frontier Energy (LIFE), Loyola College, Chennai 600034, India
e-mail: arunkumarphy@gmail.com

conductivity of TiO_2/SiO_2 nanocomposites in comparison with synthesized pure TiO_2 and SiO_2 nanoparticles.

Experimental

Synthesis of TiO_2 nanoparticles

The solution of titanium (IV) isopropoxide $Ti(OC_3H_7)_4$ was added dropwise in isopropyl alcohol and stirred for 30 min. The metal oxide gel was produced by increasing the pH by dropwise addition of 1 N NH_3 solution. The resultant solution was stirred for 24 h and kept for 1 day aging. The solution was filtered after 1 day of aging in order to remove any particulates. The precipitate was washed several times with distilled water and dried in oven for 24 h to remove the solvent. Removal of residual organics and the stabilization of the materials were carried out by calcination for 3 h at 400°C (Aguado et al. 2006).

Synthesis of SiO_2 nanoparticles

The solution of tetra-ethylorthosilicate $Si(OC_2H_5)_4$ was added dropwise in isopropyl alcohol and stirred for 30 min. The metal oxide gel was produced by increasing the pH by dropwise addition of 1 N NH_3 solution. The resultant solution was stirred for 24 h and kept for 1 day aging. The solution was filtered after 1 day of aging in order to remove any particulates. The precipitate was washed several times with distilled water and dried in oven for 24 h to remove the solvent. Removal of residual organics and the stabilization of the materials were carried out by calcination for 3 h at 400°C (Aguado et al. 2006).

Synthesis of TiO_2/SiO_2 nanocomposites

The solution of titanium (IV) isopropoxide $Ti(OC_3H_7)_4$ was added dropwise in isopropyl alcohol and stirred. A solution of tetra-ethylorthosilicate $Si(OC_2H_5)_4$ in isopropyl alcohol was added to the reaction medium and stirred for 30 min. The mixed oxide gel was produced by increasing the pH by dropwise addition of 1 N NH_3 solution. The resultant solution was stirred for 24 h and kept for 1 day aging. The solution was filtered after 1 day of aging in order to remove any particulates. The precipitate was washed several times with distilled water and dried in oven for 24 h to remove the solvent. Removal of residual organics and the stabilization of the materials were carried out by calcination for 3 h at 400°C (Aguado et al. 2006).

Characterization

The crystal structure of the powder was studied by powder X-ray diffraction with Rigaku II Cu K(α) using a Cu Kα radiation ($\lambda = 0.154$ nm). The diffraction patterns were taken over the 2θ range 20°–80° by step scanning with a step size of 0.02°. The average crystallite sizes of TiO_2, SiO_2 nanoparticles and TiO_2/SiO_2 nanocomposites were determined according to Scherrer's equation $D = 0.94\lambda/\beta \cos\theta$ (Castro et al. 2008; Bartram 1967), where D is crystallite size, λ is wavelength, β is full width half maximum, and θ is angle of diffraction. The Fourier transform infrared spectra of the samples were studied using Perkin–Elmer infrared spectrophotometer. The spectrum is recorded in the range of wavenumber 500–4,000 cm^{-1}. Nitrogen adsorption–desorption isotherm at 74 K was obtained from ASAP 2020 Micrometrics. Surface areas were determined according to the Brunauett–Emmett–Teller (BET) method. The pore size distributions were calculated by applying the Barrett–Joyner–Halenda (BJH) model. The BET surface area, micropore area, macropore volume, mesopore volume and total pore volume were calculated. The UV–Vis spectra were obtained using UV–Vis–NIR spectrophotometer. The spectra were recorded at room temperature in the range 200–1,000 nm. The field-dependent dark and photoconductivity studies were carried out using Keithley picoammeter. The experimental setup for the measurement of field-dependent dark and photoconductivity is as used by Ponniah and Xavier (2007). The samples in the form of pellets are attached to the microscopic glass slide and two electrodes of thin copper wire (0.14-mm diameter) were fixed by the use of silver paint. The ends of the copper wire were connected to DC power supply through picoammeter (Keithley picoammeter 6485) as shown in Fig. 1. The applied field was varied and the corresponding current in the circuit was measured. To measure the photocurrent, light from 100 W halogen light was illuminated onto the sample (Ponniah and Xavier 2007).

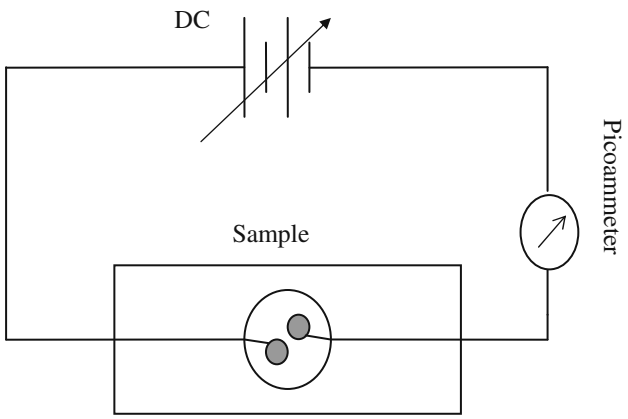

Fig. 1 Experimental set up for the measurement of field-dependent conductivity

Results and discussion

Figure 2 shows the XRD pattern of the TiO_2, SiO_2 nanoparticles and TiO_2/SiO_2 nanocomposite obtained by the sol–gel method. The XRD pattern of the as-prepared TiO_2 shows the presence of broad peak. All the diffraction lines are assigned well to the crystallite phase of TiO_2 (Zhao et al. 2007). The XRD pattern is in excellent agreement with the reference pattern (JCPDS 21-1272) of TiO_2. It should be noted that only anatase TiO_2 is detected and no rutile phase can be found in the sample (Khanna et al. 2007). The XRD pattern of prepared SiO_2 nanoparticle and TiO_2/SiO_2 nanocomposites shows the presence of very broad peak. The broad peak indicates that either the particles are of very small crystallite size, or particles are semi crystalline in nature (Yeh et al. 2004; Zhou et al. 2006). The average crystalline sizes of the as-synthesized nanoparticles were estimated from XRD line broadening using Scherrer's equation (Castro et al. 2008; Bartram 1967) by considering the full width and half maximum (FWHM) value (shown in Table 1). The crystallite size of TiO_2/SiO_2 nanocomposite is found to be 0.50 nm. This relatively low crystallite size is due to the low growth rate (Jian et al. 1991).

UV–Vis absorption study was carried out in order to characterize the optical absorbance of the sample. The absorption spectra of the as-synthesized TiO_2, SiO_2 nanoparticles and TiO_2/SiO_2 nanocomposite are shown in Figs. 3, 4 and 5, respectively. The optical band gap can be

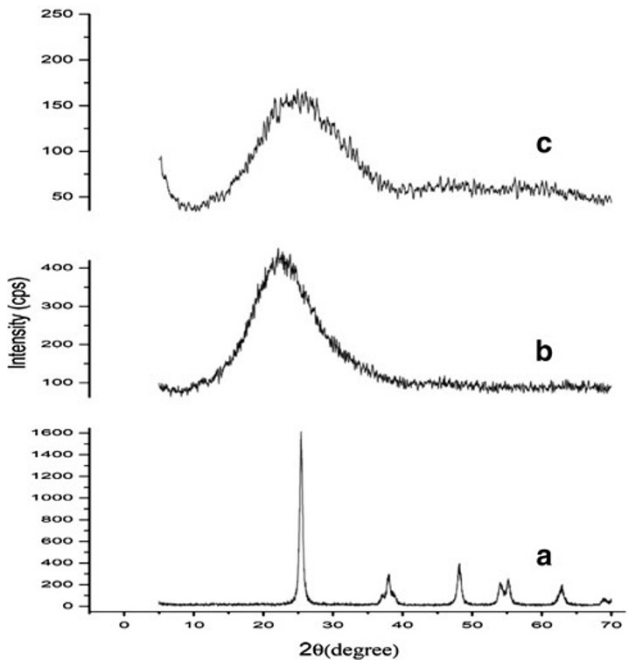

Fig. 2 XRD pattern of the as-synthesized mesoporous **a** TiO_2 nanoparticles, **b** SiO_2 nanoparticles and **c** TiO_2/SiO_2 nanocomposite

Table 1 Particle size and optical band gap of the as-synthesized samples

Sample	2θ (degree)	β (rad)	Crystallite size (nm)	E_g (eV)
TiO_2	25.38	0.029656	4.74	3.54
SiO_2	22.42	0.22242	0.63	3.85
TiO_2/SiO_2	25.48	0.281553	0.50	3.35

B Full width half maximum, θ angle of diffraction, E_g optical band gap

estimated by plotting $(\alpha hv)^2$ versus photon energy (hv) based on the relation $\alpha hv = A\,(hv - E_g)^{n/2}$ where α is the absorption coefficient, A is a constant, E_g is the band gap and n is the exponent depending on quantum selection rule for a particular material, $n = 1$ for a direct transition (Khanna et al. 2007; Oral et al. 2004). According to the above relation, the intercept of the tangent on the photon energy axis corresponds to optical band gap (Oral et al. 2004). From the $(\alpha hv)^2$ versus photon energy (hv) plots, the optical band gaps E_g for all the three synthesized samples were estimated and tabulated in Table 1. Figure 6 shows the UV–Vis spectrum of the as-synthesized samples. All the three as-synthesized samples show similar absorption pattern in which the TiO_2/SiO_2 nanocomposite shows better absorbance in visible range compared to TiO_2 and SiO_2 nanoparticles.

Nitrogen adsorption isotherm pattern of the as-synthesized mesoporous TiO_2, SiO_2 nanoparticles and TiO_2/SiO_2 nanocomposites is shown in Figs. 7, 8 and 9, respectively. Some characteristics of the samples, such as BET surface area, micropore area, average pore diameter, micropore volume, mesopore volume and total pore volume are listed in Table 2. According to IUPAC nomenclature, the

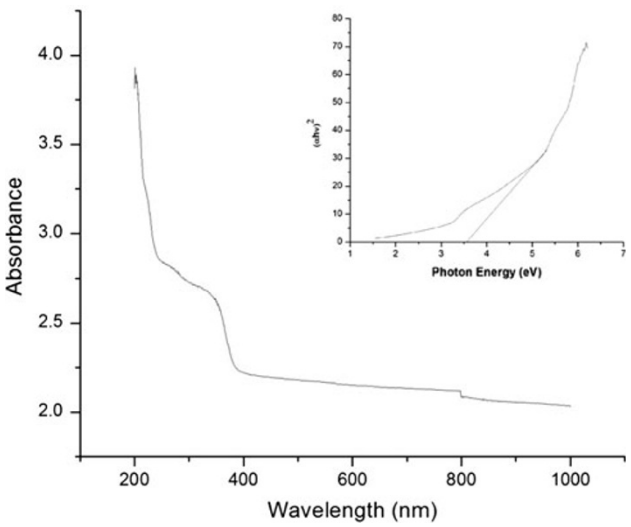

Fig. 3 UV-Vis spectrum of the as-synthesized TiO_2 nanoparticles *inset* shows the corresponding plot of photon energy versus $(\alpha hv)^2$

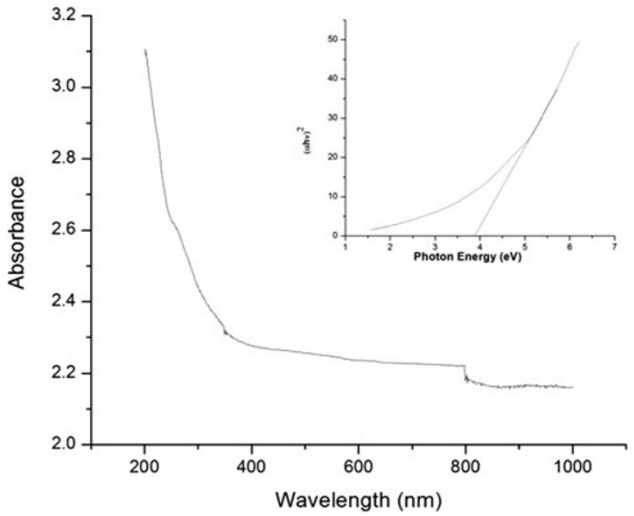

Fig. 4 UV-Vis spectrum of the as-synthesized SiO_2 nanoparticles *inset* shows the corresponding plot of photon energy versus $(\alpha hv)^2$

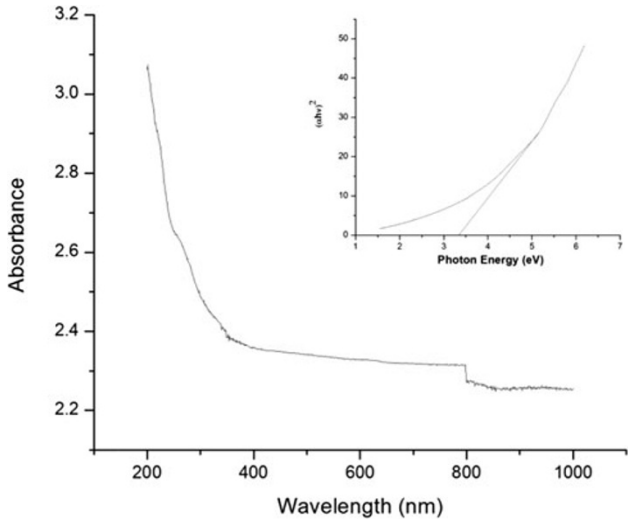

Fig. 5 UV-Vis spectrum of the as-synthesized TiO_2/SiO_2 nanocomposite *inset* shows the corresponding plot of photon energy versus $(\alpha hv)^2$

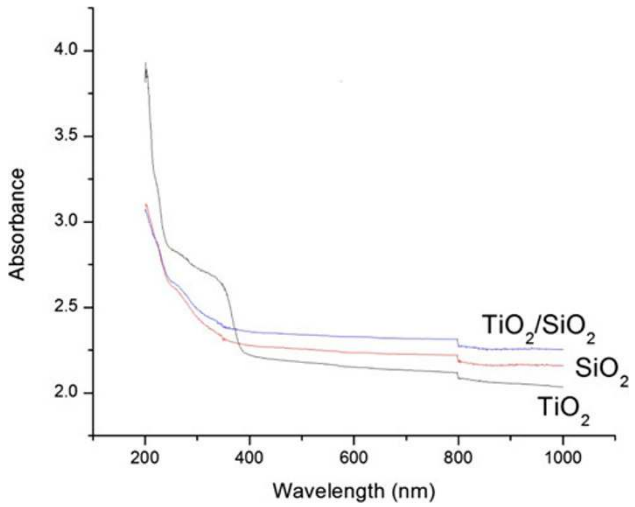

Fig. 6 UV-Vis spectrum of the as-synthesized TiO_2, SiO_2 nanoparticles and TiO_2/SiO_2 nanocomposite

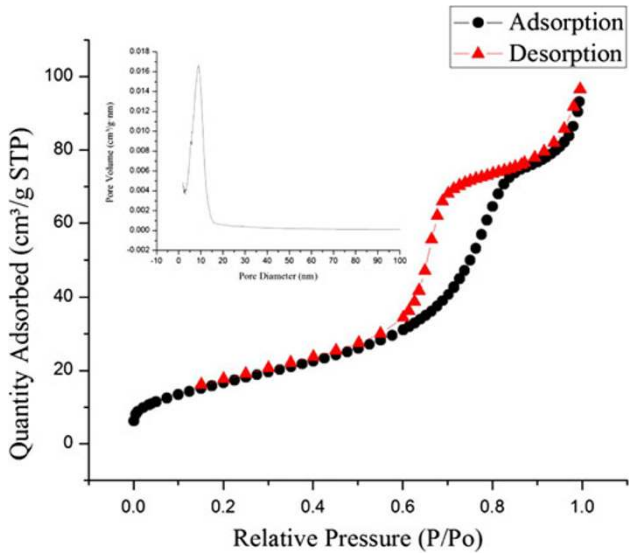

Fig. 7 Nitrogen adsorption isotherm pattern of TiO_2 nanoparticle (*inset* pore size distribution)

absorbent pores are classified into three groups: micropore (diameter <2 nm), mesopore (diameter 2–50 nm) and macropore (diameter >50 nm) (Wang et al. 2010). The BET measurements confirmed the absence of macropores in all nanoparticles. The pore diameter for TiO_2, SiO_2 nanoparticle and TiO_2/SiO_2 nanocomposite was found to be 8.39, 9.32 and 9.82 nm. The mesopore volume was obtained by subtracting micropore volume from the corresponding total volume (Sayilkan et al. 2007). The mesoporosities (percentage of mesopore to total pore volume V_{mes}/V_{tot}) were calculated and found to be 75.45, 73.8 and 50.53% for TiO_2, SiO_2 nanoparticle and TiO_2/SiO_2 nanocomposite, respectively. For TiO_2/SiO_2 nanocomposites, the microporosity increased and the mesoporosity decreased when compared to TiO_2 and SiO_2 nanoparticles. This may be due to shrinking of mesopores or due to the SiO_2 being absorbed into the mesopores of TiO_2 (Sayilkan et al. 2007). The BET surface area was found to be 62 to 303 m^2/g in the case of TiO_2 nanoparticles and TiO_2/SiO_2 nanocomposite, respectively. This sizeable increase in surface area of TiO_2/SiO_2 nanocomposite may be due to the SiO_2 limiting the agglomeration of TiO_2 particles (Nilchi et al. 2011; Sirimahachai and Ndiege 2010).

Fourier transform infrared (FTIR) spectrum of as-synthesized mesoporous TiO_2 nanoparticles is shown in Fig. 10. It was absorbed that the strong band in the range of 900–500 cm^{-1} is associated with the characteristic vibrational modes of TiO_2 (Khanna et al. 2007). This confirms

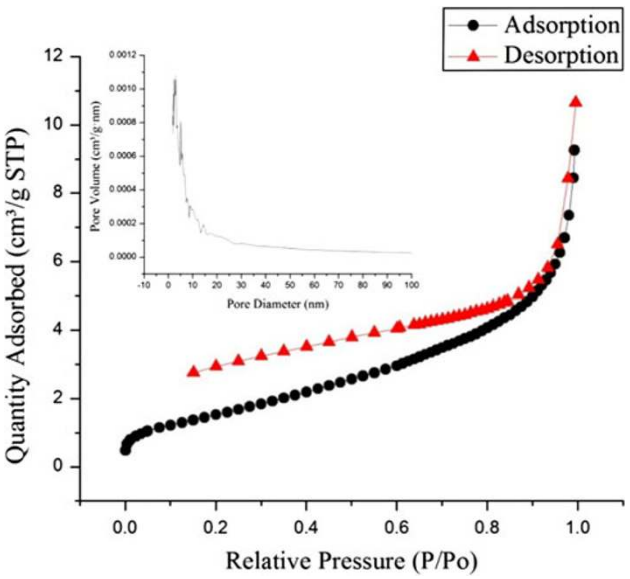

Fig. 8 Nitrogen adsorption isotherm pattern of SiO_2 nanoparticle *inset* pore size distribution

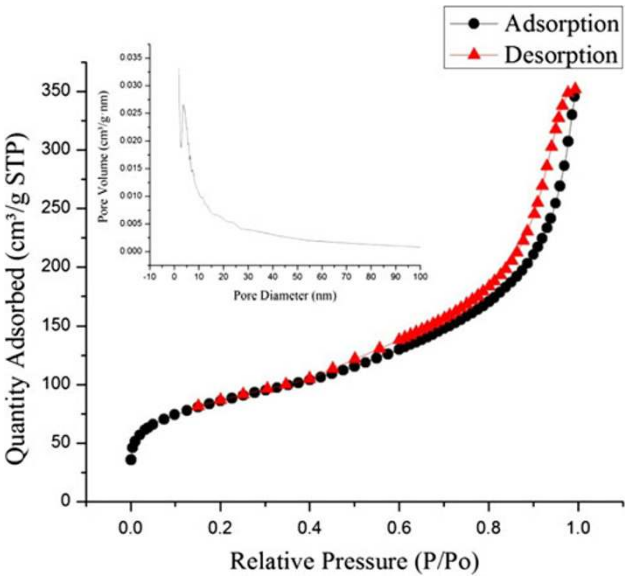

Fig. 9 Nitrogen adsorption isotherm pattern of TiO_2/SiO_2 nanocomposite *inset* pore size distribution

that the TiO_2 phase has been formed. The absorption in the range from 3,640 to 2,500 cm^{-1} may be related to the presence of O–H stretching vibration (Monomer, intermolecular, intramolecular and polymeric). The absorption band at 1,629 cm^{-1} was due to the presence of O–H bending vibration which is probably because the reabsorption of water from the atmosphere has occurred (Mohan 2009). Fourier transform infrared spectrum of as-synthesized mesoporous SiO_2 nanoparticles is shown in Fig. 11. The two strong bands 1,118 and 804 cm^{-1} observed are associated with asymmetric and symmetric Si–O–Si stretching vibrations (Aziz and Sopyan 2009), respectively. This confirms that the SiO_2 phase is formed. FTIR also showed that the band at 1,076 cm^{-1} was slightly shifted towards lower wavenumber as the particle size is reduced (Singh et al. 2011). The absorption bands at 3,428 and 1,635 cm^{-1} were due to the presence of O–H stretching and bending vibrations (Mohan 2009), respectively. Fourier transform infrared (FTIR) spectrum of as-synthesized mesoporous TiO_2/SiO_2 nanocomposite is shown in Fig. 12. The band observed at 923 cm^{-1} is associated with Si–O–Ti vibration (Aziz and Sopyan 2009). The two strong bands at 1,050 and 803 cm^{-1} observed are associated with asymmetric and symmetric Si–O–Si stretching vibration (Aziz and Sopyan 2009), respectively. The strong bands in the range 900–500 cm^{-1} are associated with vibrational modes of TiO_2. The absorption bands at 3,419 and 1,631 cm^{-1} were due to the presence of O–H stretching and bending vibrations (Aziz and Sopyan 2009), respectively.

The field-dependent dark and photoconductivity of TiO_2, SiO_2 nanoparticles and TiO_2/SiO_2 nanocomposite are shown in Figs. 13 and 14, respectively. The plot indicates a linear increase of current in the dark and visible light-illuminated samples in all the three cases with increase in applied field depicting the ohmic nature of the contacts (Dhar and Chakrabarti 1996). TiO_2/SiO_2 nanocomposite showed better dark and photo currents compared to TiO_2 and SiO_2 nanoparticles. For example, for a fixed field of 800 V/cm, the TiO_2, SiO_2 nanoparticles and TiO_2/SiO_2 nanocomposite showed dark current of 0.0178, 0.4 and 4.607 μA, respectively. It is 258 fold more than the value for TiO_2 nanoparticle. For a fixed field of 800 V/cm, the TiO_2, SiO_2 nanoparticles and TiO_2/SiO_2 nanocomposite

Table 2 The physical properties of the as-synthesized samples

Sample	Crystallite size (nm)	S_{BET} (m^2/g)	A_{mic} (m^2/g)	P_{dia} (nm)	V_{mic} (cm^3/g)	V_{mes} (cm^3/g)	V_{tot} (cm^3/g)	V_{mic}/V_{tot} (%)	V_{mes}/V_{tot} (%)
TiO_2	4.74	62.181	53.642	8.39	0.02624	0.08065	0.1069	24.54	75.45
SiO_2	0.63	5.7189	4.8534	9.32	0.00248	0.00697	0.0095	26.20	73.8
TiO_2/SiO_2	0.50	302.99	318.07	9.82	0.15706	0.16044	0.3175	49.47	50.53

S_{BET} BET surface area, A_{mic} micropore surface area, V_{mic} micropore volume V_{mes} mesopore volume, V_{tot} total pore volume, P_{dia} BJH average pore diameter

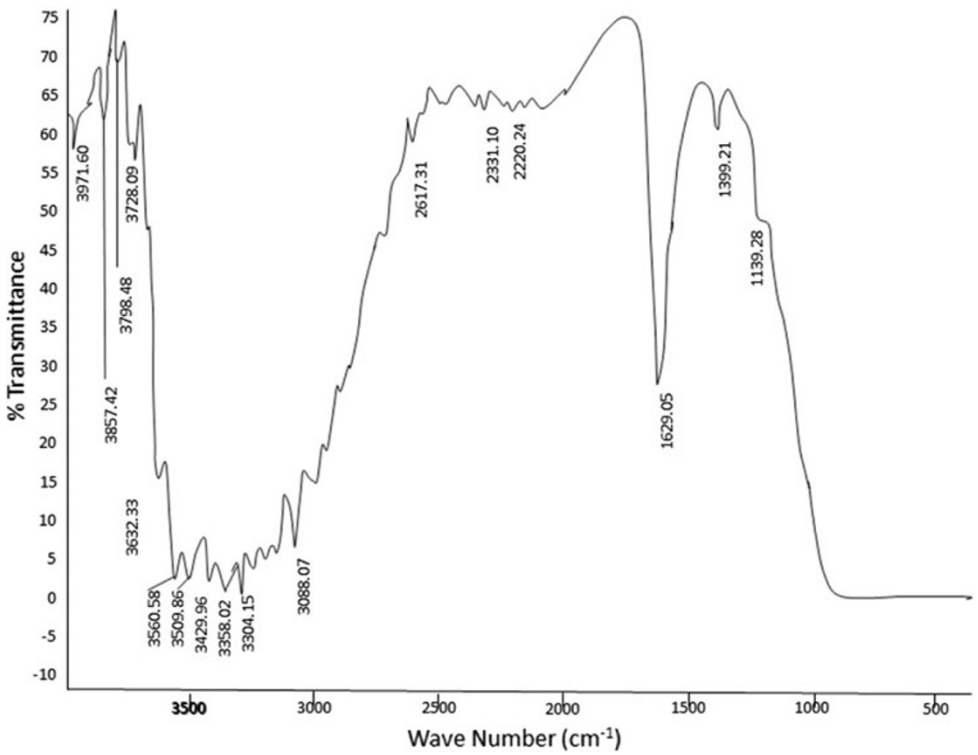

Fig. 10 FTIR spectrum of as-synthesized TiO_2 nanoparticles

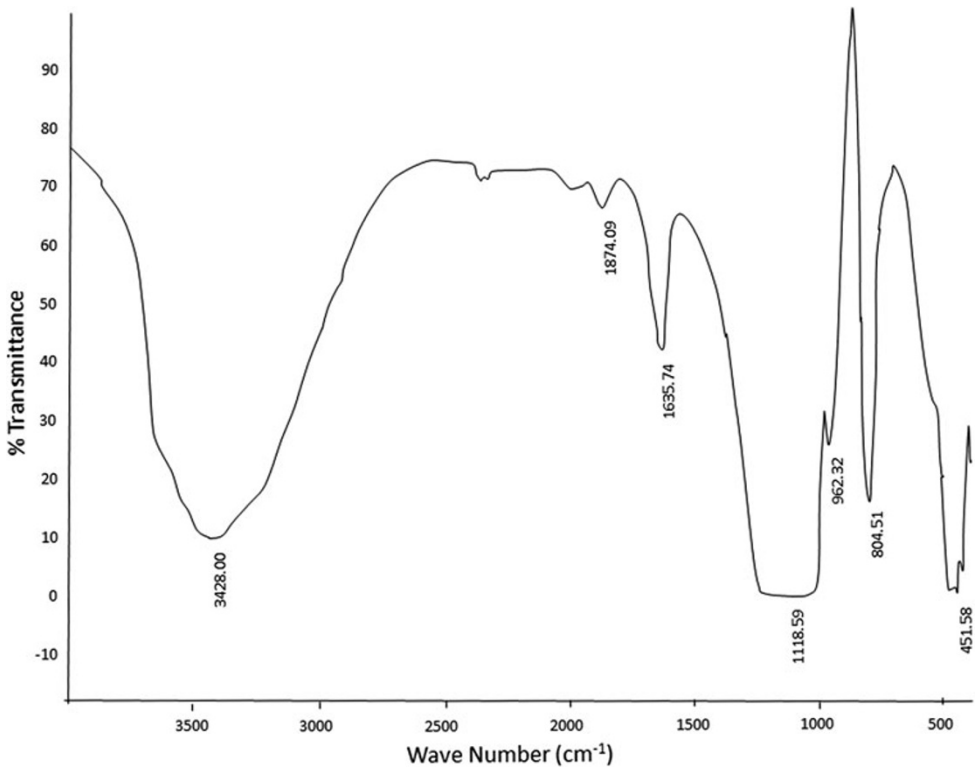

Fig. 11 FTIR spectrum of as-synthesized SiO_2 nanoparticles

showed dark current of 0.0191, 0.5 and 5.6375 μA, respectively. It is nearly 300 times more the value of TiO_2 nanoparticle. This may be due to the enhanced surface area available for conduction or attributed to the increase in charge carrier concentration and drift mobility in the composite (Xavier and Goldsmith 1995).

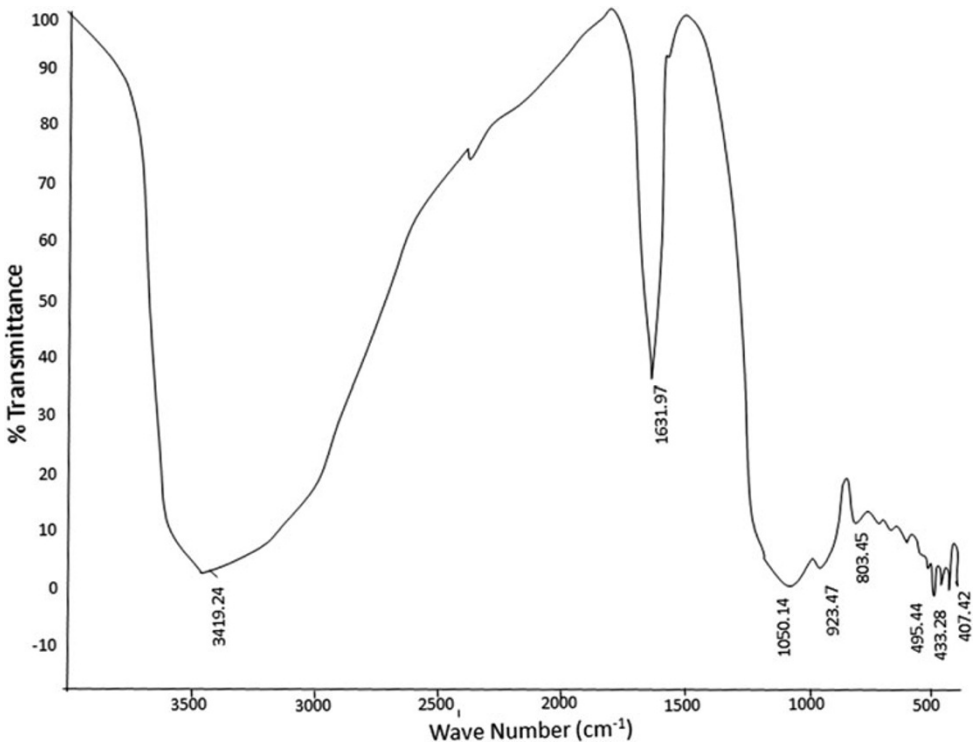

Fig. 12 FTIR spectrum of as-synthesized TiO_2/SiO_2 nanocomposite

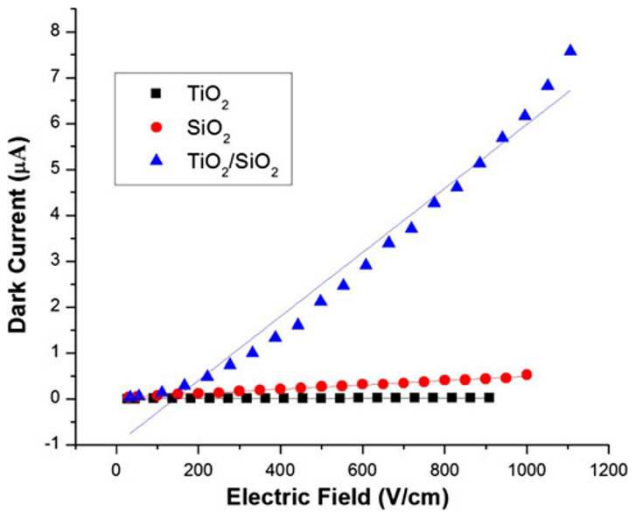

Fig. 13 The field-dependent dark conductivity of as-synthesized mesoporous TiO_2, SiO_2 nanoparticles and TiO_2/SiO_2 nanocomposite

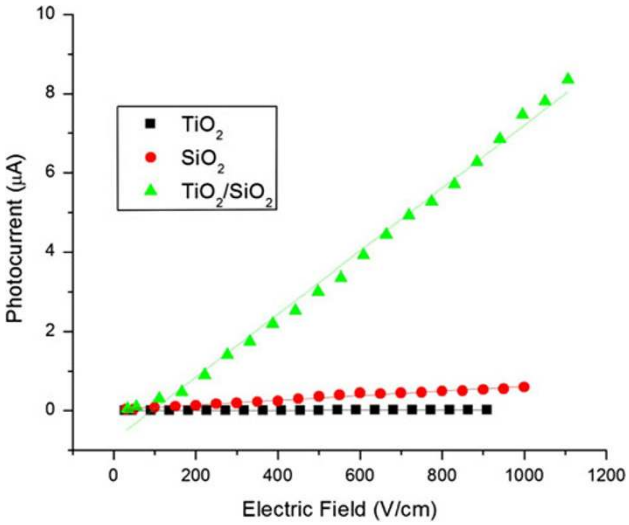

Fig. 14 The field-dependent photoconductivity of as-synthesized mesoporous TiO_2, SiO_2 nanoparticles and TiO_2/SiO_2 nanocomposite

Conclusion

A novel, easy and reproductive method was followed for the synthesis of TiO_2, SiO_2 nanoparticles and TiO_2/SiO_2 nanocomposites. TiO_2/SiO_2 nanocomposite showed enhanced surface area of 303 m^2/g in comparison with TiO_2 nanoparticle which increases the photocurrent in the field-dependent photoconductivity. The pore size distribution shows that the as-synthesized nanocomposite is mesoporous. The material with large surface area and mesoporous nature would increase the adsorption of dye on it, which in turn will improve photosensitivity to solar radiation. Thus, TiO_2/SiO_2 nanocomposites can be dye sensitized and used as working electrode in dye-sensitized solar cells.

Acknowledgments The authors thank Dr. B. Viswanathan, National Centre for Calalysis Research, Indian Institute of Technology, Madras for providing with XRD and BET facilities and Dr. A. R. Phani, Managing Director, Nano-RAM Technologies for constant support in experimental part. The authors are grateful to the Research team of Loyola Institute of Frontier Energy (LIFE) for the financial and moral support rendered to complete this work.

References

Aguado J, Grieken RV et al (2006) Comprehensive study of the synthesis characterization and activity of TiO_2 and mixed TiO_2/SiO_2 photo catalyst. Appl Catal A: Gen 312:202–212

Aziz RA, Sopyan I (2009) Synthesis of TiO_2-SiO_2 powder and thin film photocatalysts of sol-gel method. Int J Chem 48:951–957

Bartram SF (1967) Handbook of X-rays. In: Kaelble EF (ed). McGraw-Hill, New York, pp 1–17

Castro AL, Nunes MR et al (2008) Synthesis of anatase TiO_2 nanoparticle with high temperature stability and photoconductivity activity. Solid State Sci 10:602–606

Dhar S, Chakrabarti S (1996) Electroless Ni plating on *n* and *p*-type porous silicon Si for ohmic and rectifying contacts. Semicond Sci Technol 11:1231. doi:10.1088/0268-1242/11/8/020

Hakki A, Dillert R, Bahnemann D (2009) Photocatalytic conversion of nitroaromatic compound in the presence of TiO_2. Catal Today 144:154–159

Jian L, Vizkelethy G, Revesz P, Mayer JW, Tu KN (1991) Oxidation and reduction of copper oxide thin films. J Appl Phys 69: 1020–1029

Khanna PK, Singh N, Charan S (2007) Synthesis of nanoparticles of anatase TiO_2 and preparation of its optical transparent film in PVA. Mater Lett 61:4725–4730

Mohan J (2009) Organic spectroscopy principles and applications, 2nd edn. Narosha Publishing House Pvt. Ltd, New Delhi, pp 28–95

Nilchi A, Janitabar-Darzi S, Rasouli-Garmarodi S (2011) Sol-gel preparation of nanoscale TiO_2/SiO_2 composite for eliminating of con red azo dye. Mater Sci Appl 2:476–480

Ohno T, Tagawa S et al (2009) Size effect of TiO_2-SiO_2 nanohybrid particle. Mater Chem Phys 113:119–123

Oral AY, Mensur E, Aslan MH, Basaran E (2004) The preparation of copper(II) oxide thin films and the study of their microstructures and optical properties. Mater Chem Phys 83:140–144

Ponniah D, Xavier F (2007) Electrical and electroreflectance studies on ortho-chloranil-doped polyanaline. Physica B 392:20–28

Rufen C, Huating L (2011) Preparation of Cr-doped TiO_2/SiO_2 photocatalysts and their photocatalytic properties. J Chin Chem Soc 58:1–8

San Vicente G, Morales A, Gutierrez MT (2001) Preparation and characterization of sol-gel TiO2 antireflective coatings for silicon. Thin Solid Films 391:133–137

Sayilkan F, Asilturk M et al (2007) Hydrothermal synthesis, characterization and photocatalytic activity of nanosized TiO_2 based catalysts for rhodamine B degradation. Turk J Chem 31: 211–221

Singh LP, Agarwal SK, Bhattacharyya SK, Sharma U, Ahalawat S (2011) Preparation of silica nanoparticles and its beneficial role in cementitious materials. Nanomater Nanotechnol 1:44–51

Sirimahachai U, Ndiege N (2010) Nanosized TiO_2 particles decorated on SiO_2 spheres (TiO_2/SiO_2): synthesis and photocatalytic activities. J Sol-Gel Sci Technol 56:53–60. doi:10.1007/s10971-010-2272-z

Wang L, Zhang J, Zhao Ran, Li Cong, Li Ye, Zhang Chenglu (2010) Adsorption of basic dyes on activated carbon prepared from polygonum orientale Linn: Equilibrium, kinetic and thermodynamic studies. Desalination 254:68–74

Xavier FP, Goldsmith GJ (1995) Photoconductivity of iodine doped single crystals of phthalocyanine. Bull Mater Sci 18:283–287

Yeh CL, Yeh SH, Ma HK (2004) Flame synthesis of titania particles from titanium tetraisopropoxide in premixed flames. Powder Technol 145:1–9

Zhang J, Xu K (2004) Valence electron structure analysis of crystalline orientation in plasma oriented in plasma sprayed TiO_2 coating. Appl Surf Sci 221:1–3

Zhao Y, Chunzhong Li et al (2007) Synthesis and optical properties of TiO_2 nanoparticles. Mater Lett 61:79–83

Zhou L, Yan S et al (2006) Preparation of TiO_2–SiO_2 film with high photocatalytic activity on PET substrate. Mater Lett 60:396–399